Uludağ University Journal of The Faculty of Engineering, Vol. 24, No. 2, 2019 RESEARCH

DOI: 10.17482/uumfd.560358

INVESTIGATION OF THE EFFECTS OF SOME PROCESS PARAMETERS ON THE MORPHOLOGICAL PROPERTIES OF POLYURETHANE NANOFIBROUS MATS CONTAINING BLACK SEED OIL

Cansu ARAS [*]
Şebnem DÜZYER GEBİZLİ [*]
Elif TÜMAY ÖZER [**]
Esra KARACA [*]

Alınma: 03.05.2019 ; düzeltme: 25.06.2019 ; kabul: 27.06.2019

Abstract: Black seed and its extracts have been used in alternative medicine since ancient times. The aim of this study is to produce and characterize composite nanofibrous surfaces by electrospinning with the addition of black seed oil (BSO) with different concentrations into the thermoplastic polyurethane polymer for wound dressings. During electrospinning the flow rate, and the distance between the needle and the collector were changed. The morphologies of the surfaces were analyzed by scanning electron microscopy (SEM). The nanofiber diameters, pore size and porosity of the nanofibrous mats were determined. The presence of black seed oil was investigated by FTIR analysis and the wettability of the surfaces was examined by contact angle measurements. As a result, optimum electrospinning process parameters and the most appropriate black seed oil concentration were determined to produce continuous, uniform and bead-free nanofibers.

Keywords: Polyurethane, black seed oil, electrospinning, composite nanofiber

Çörekotu Yağı İçeren Poliüretan Nanolifli Yüzeylerin Morfolojik Özellikleri Üzerine Bazı Proses Parametrelerinin Etkilerinin Araştırılması

Öz: Çörekotu tohumu ve ondan elde edilen ekstraktlar antik çağlardan beri alternatif tıp alanlarında uygulanmaktadır. Bu çalışmada, termoplastik poliüretan polimeri içerisine farklı konsantrasyonlarda çörek otu yağı ilave edilerek, elektro çekim yöntemi ile yara örtüsü amaçlı nanolifli kompozit yüzeyler üretilmesi ve karakterize edilmesi amaçlanmıştır. Üretim esnasında besleme ünitesi ile toplayıcı arasındaki mesafe ve besleme oranı değiştirilerek; elde edilen yüzeylerin morfolojileri taramalı elektron mikroskopu (SEM) ile analiz edilmiştir. Nanolifli yüzeylerin, nanolif çapı, gözenek boyutu ve gözeneklilikleri tayin edilmiştir. Nanolifli yapı içerisindeki çörek otu yağının varlığı FTIR analizi ile ve yüzeylerin ıslanabilirlik seviyesi temas açısı ölçümleri ile incelenmiştir. Sonuç olarak; sürekli, üniform ve boncuk içermeyen nanolifler elde etmek için çörekotu yağı katkısı için en uygun konsantrasyon ve optimum elektro çekim proses parametreleri belirlenmiştir.

Anahtar Kelimeler: Poliüretan, çörekotu yağı, elektro çekim, kompozit nanolif

[*] Bursa Uludag University, Faculty of Engineering, Textile Engineering Department, 16059, Gorukle, Bursa
[**] Bursa Uludag University, Faculty of Arts and Sciences, Chemistry Department, 16059, Gorukle, Bursa
Corresponding Author: Esra Karaca (ekaraca@uludag.edu.tr)
This study is a part of the master thesis of the first author

1. INTRODUCTION

Nigella Sativa (NS), commonly known as "black seed", is an herbaceous plant that grows around of Mediterranean countries (Zaoui et al., 2002). The black seed and its extracts have the wide variety of applications in the traditional medicine and it can be use on treatment of various diseases including diabetes, asthma, flatulence, polio, kidney stones, and abdominal pains. Many pharmacological studies have been conducted to investigate its biological activities and therapeutic properties such as analgesic and anti-inflammatory effect (Hajhashemi et al., 2004), anti-cancer (Gali-Muhtasib et al., 2006), antibacterial activity (Randhawa et al., 2016), anti-fungal effect (Aljabre et al., 2005), anti-oxidant effect (Burits and Bucar, 2000). Main components of black seed oil (BSO) are saturated/unsatured fixed oil, essential oil (0.4-0.45%), carbohydrate (33-34%), protein (16-19.9%), amino acid, alkaloid, tannins, saponins, minerals (calcium, zinc, phosphate), vitamins (ascorbic acid, thiamine, niacin, pyridoxine and folic acid) (Güzelsoy et al., 2018). The thymoquinone, which is known to cause for many therapeutic properties, is a major active chemical component (30%-48%) of essential oil of the black seed (Ahmad et al., 2013). Many studies have been also issued to prove therapeutic effects of thymoquinone (Kalhori et al., 2018; Majdalawieh, 2017).

Polymeric nanofibers possess unique properties, such as ultra-fine fiber diameter, high surface area per unit mass, high porosity, small pore size, high mechanical properties, and extreme flexibility depending on the polymer structure. Therefore, they are favorable for many applications (Akduman and Kumabasar, 2017 and Mi et al., 2015). Electrospinning is an effective method for the production of polymer nanofibers with the usage of electrostatical forces. In this method, a droplet of a polymer solution is subjected to an electrical field. With the increasing voltage, the solvent evaporates, leaving behind a mat of dry polymeric nanofibers on the collector (Tijing et al., 2012; Almetwally et al., 2017).

Due to their outstanding properties, nanofibrous mats present a wide range of application possibilities from agriculture to protective clothing. Among many application areas, nanofibrous mats are promising for medical applications such as tissue engineering, drug delivery, wound healing, tumor therapy, and barrier textiles due to their small fiber diameter, high surface area to volume ratio, small pore size, high porosity and high mechanical properties (Huang, et al., 2003; Chronakis, 2005).

Although electrospinning is relatively a simple method compared to other nanofiber production methods, there are many parameters affecting the morphology of the nanofibers. These parameters are mainly solution parameters (viscosity, surface tension, pH, molecular weight of the polymer, etc.), process parameters (flow rate, spinning distance, voltage, needle diameter, etc.) and ambient parameters (temperature and humidity). In order to produce an appropriate nanofibrous mat with desired properties, these parameters should be carefully selected (Teo and Ramakrishna, 2006; Theron et al., 2004).

Polyurethane (PU) is a highly used polymer in medical applications because of their biocompatible nature, non-toxicity, controlled degradation, good barrier properties and capability of gas and water permeability (Detta et al.,2010). They are a type of polyurethane (PU) composed of chemical reaction between isocyanates (hard segments) and polyols (soft segments) and contain repeating urethane groups (Sharmin and Zafar, 2012). They also have high elongation, good mechanical properties, water insolubility, abrasion and tear resistance properties (Akduman et al., 2016). There are many studies reported in the literature on the medical applications of PU nanofibers as vascular grafts (Theron et al., 2010), coating materials for implantable biosensors and stents (Wang et al., 2018; Pant et al., 2015), tissue engineering applications (Mi et al., 2014), heart valve (Chen et al., 2009), drug delivery systems (Saha et al., 2014), wound healing applications (Hacker et al., 2013; Tan et al., 2015; Guo et al., 2012), etc. Recently, various researches have been focused on developing wound dressings blended with essential oils such as murivenna, rosemary, oregano, cinnamon (Manikandan, et al., 2017, Rieger and Schiffman, 2014; Liakos et al., 2017; Wen et al., 2016). However, to the best of our

knowledge, there is no research explaining production and characteristics of PU nanofibrous mats containing black seed oil.

The aim of this study is to produce PU/BSO nanofibrous mats by electrospinning, to determine the optimum solution and process parameters (flow rate and spinning distance) for the electrospinning of PU/black seed oil nanofibers, and to investigate the effect of solution properties and process parameters on the morphology of PU/BSO nanofibrous mats. Therefore, PU/BSO solutions with different concentrations were prepared. The solutions were characterized in terms of viscosity, pH and surface tension. PU/BSO nanofibers were produced by using single needle electrospinning process with different flow rates and spinning distances. The surface properties were investigated by Scanning Electron Microscopy (SEM) studies and contact angle measurements. Fourier Transform Infrared spectrometry (FTIR) analyses were performed in order to understand the chemical structure of the fibers. SEM studies showed that PU and PU/BSO nanofibers were successfully with diameters mostly below 500 nm. The diameters and contact angle values were slightly decreased depending on the BSO content in the nanofibrous mat. It was also seen that; process parameters have significant effect on the mat morphologies.

2. MATERIALS AND METHODS

2.1 Materials

To prepare PU and PU/BSO electrospinning solutions, polyester-based thermoplastic PU (BASF Elastollan®) with a molecular weight of 107.010 g/mol and a bulk density of 1.19 g/cm^3 was used. Cold pressed black seed oil was supplied from a local farmer in Bursa-Mustafakemalpaşa (Turkey). Dimethylformamide (DMF) (Sigma-Aldrich, USA) was used as solvent to prepare the spinning solutions. All the chemicals were used as received without any further purification.

2.2 Methods

2.2.1 Production of PU and PU/BSO nanofibrous mats

Prior to the solvent preparation, the fatty acid composition of black seed oil was determined. Analysis of fatty acid composition of black seed oil was carried out using an Agilent 6890 N GC gas chromatography-flame ionization dedector (GC–FID) (Agilent Technologies, Palo Alto, CA). An HP-88 fused-silica capillary column 100m×0.25 i.d., with 0.20 um film thickness was employed. The injector temperature was set at 250 °C. The GC oven temperature was held at 120 °C for 1 min, then increased to 175 °C at a heating rate of 10 °C min^{-1}, 210 °C at a heating rate of 3 °C min^{-1}, 240 °C at a heating rate of 5 °C min^{-1} and the temperature was held for 5min. Standard test method of TS EN ISO 12966-2 and TS EN ISO 12966-4 was used in analysis. The test was repeated three times.

In this study, three different solutions were prepared with 5%, 10%, and 15% (v/v) BSO addition into the spinning solution. PU solutions without addition of BSO were also prepared as reference. In order to prepare PU/BSO electrospinning solutions, 10% (w/v) PU and BSO with different concentrations were dissolved in DMF and stirred at room temperature for 24 h. For the sake of brevity, the reference sample was denoted as PU, while the solutions with different BSO concentrations were denoted as PU/BSO5, PU/BSO10, and PU/BSO15.

The prepared solutions and pure black seed oil were characterized in terms of viscosity, surface tension, and pH. The viscosities of all solutions were determined by Brookefield viscometer at 100 rpm. Surface tension values of the solutions were measured by KSV-The Modular CAM 200 tensiometer and the pH values were determined by a Hanna pH tester.

Electrospinning was performed with an Inovenso Electrospinning Equipment. All experiments were carried out 15 kV at room temperature. The nanofibrous mats were collected

on a rotating drum with a speed of 200 rpm. All electrospun mats were produced from electrospinning solutions of 20 mL. The details of the process are given in Table 1.

Table 1. The electrospinning parameters

PU concentration (%)	BSO concentration (%)	Flow rate (mL/h)	Distance (cm)	Sample ID
10	-	0.5	18	PU-1
			20	PU-2
		0.7	18	PU-3
			20	PU-4
	5	0.5	18	PU/BSO5-1
			20	PU/BSO5-2
		0.7	18	PU/BSO5-3
			20	PU/BSO5-4
	10	0.5	18	PU/BSO10-1
			20	PU/BSO10-2
		0.7	18	PU/BSO10-3
			20	PU/BSO10-4
	15	0.5	18	PU/BSO15-1
			20	PU/BSO15-2
		0.7	18	PU/BSO15-3
			20	PU/BSO15-4

2.2.2 Characterization of the PU and PU/BSO nanofibrous mats

SEM studies

The surface morphologies of the nanofibrous mats were examined by a Scanning Electron Microscope (SEM) (Carl Zeiss Evo 40). Fiber uniformity, fiber diameter distribution, fiber evenness in the mats was observed. The surfaces were coated with a thin conducted gold layer prior to SEM observations. Fiber diameters were calculated from the SEM images by measuring 100 random diameters using image analysis software (Image J).

Pore Size and Porosity Calculations

In order to calculate pore size and porosity, the samples were cut as 2x2 cm^2. Afterwards the samples were weighted by a digital scale and the thicknesses of the samples were measured by a digital micrometer. The measurements were repeated three times.
The mean effective pore diameter (pore size) and porosity of the electrospun nanofibrous mats were calculated using the following equations (Zhu et al., 2015; Ma et al., 2005; Düzyer, 2017):

$$\varepsilon = (1 - \rho e/\rho f) \times 100 \quad \ldots\ldots (1)$$

Where ε is the porosity of the electrospun nanofibrous mat, ρe and ρf are the electrospun nanofibrous mat density and bulk PU density, respectively.

$$D = \pi d/4(1-\varepsilon) \quad \ldots\ldots (2)$$

Where D is the mean effective pore diameter, d is the mean nanofiber diameter and ε is the mean porosity of the sample.

Contact Angle Measurements

The contact angle values of the electrospun nanofibrous mats were determined using KSV-The Modular CAM 200 Contact Angle Measurement System. A water droplet was dispersed on each sample by a micropipette, and the images were captured as quickly as possible after water droplet was placed onto the sample surface. Three measurements were performed on each sample and mean values were recorded.

ATR-FTIR analysis

A Perkin–Elmer Spectrum 100 FTIR Spectrometer (Perkin Elmer, Waltham, MA, USA) equipped with an attenuated total reflectance (ATR) apparatus was used to obtain FTIR spectra of oil, PU and PU/BSO nanofibrous mats within the range of 600-4000 cm^{-1} with the resolution of 2 cm^{-1}.

3. RESULTS AND DISCUSSION

3.1. Characterization of PU, BSO and PU/BSO solutions

Solution parameters play a key role on the morphology of the nanofibers. Table 2 shows the properties of the BSO, PU and PU/BSO solutions.

Viscosity of a solution is dependent on the chain entanglements in the solution. In electrospinning, a critical chain entanglement is required to obtain nanofibers (Mi et al., 2013, Ramakrishna et al., 2005). It can be seen that, BSO addition into the spinning solution resulted in higher viscosities due to the increase in polymer concentration per unit area at a constant volume.

Surface tension of the polymer solution directly affects polymer jet formation, as the electrostatic forces in the electric field must overcome the surface tension of the solution to form a polymer jet (Teo and Ramakrishna, 2006). With the BSO addition into the spinning solution, the surface tension values of the solutions were slightly increased indicating that higher electrical forces are needed to overcome the surface tension of the polymer droplet at the spinneret (Demir et al., 2001). This result is also compatible with the viscosity increase of the solutions.

Since pure BSO has an acidic nature, the pH of the PU/BSO solutions have slightly decreased, compared to pure PU solution. Adding an acidic component into the spinning solution leads to increase in the conductivity of the solution because of the increase in the number of ions. This may affect the diameter of the nanofibers. Thinner nanofibers can be produced from the more conductive solutions (Ramakrishna et al., 2005).

Table 2. The solution properties

Solution	Viscosity (cP)	Surface tension (mN/m)	pH
BSO	38.4	33.29	5.73
PU	1213	35.24	10.36
PU/BSO5	1295	35.97	9.41
PU/BSO10	1451	35.44	9.27
PU/BSO15	1533	38.40	9.10

3.2. Characterization of PU and PU/BSO nanofibrous mats

The nanofibrous mats (Figure 1) were successfully produced from solutions of PU and PU/BSO by electrospinning. The properties of the electrospun nanofibrous mats were given in Table 3. Generally, PU nanofibers without BSO had diameters between 400-700 nm. The increase in viscosity of the solution leads an increase in diameter (Ramakrishna et al., 2005).With the addition of BSO, the viscosities of the solutions were increased. When the

concentration of BSO in the solution was increased, the fiber diameters increased. However, PU/BSO nanofibers showed smaller diameters than PU nanofibers. This is maybe due to the pH change in the spinning solution. Since the number of ions increased with the addition of BSO, the diameters were decreased.

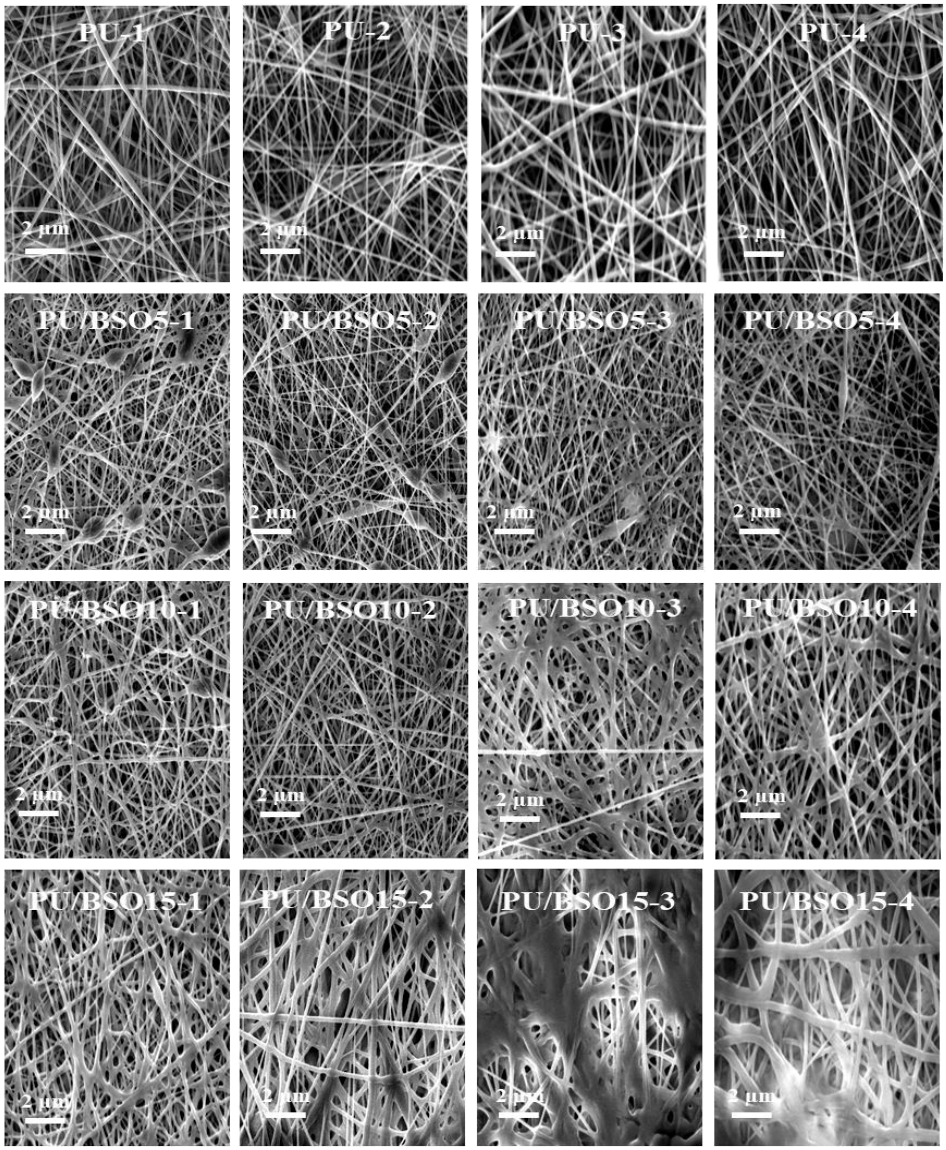

Figure 1:
SEM images of the nanofibrous mats

Table 3. The properties of the nanofibrous mats

Sample	Diameter (nm)	Pore size (µm)	Porosity (%)	Contact angle (°)
PU-1	474 ± 98	0.89	58	106.3 ± 4.3
PU-2	408 ± 98	1.90	83	103.5 ± 7.9
PU-3	719 ± 94	3.24	83	114.1 ± 2.8
PU-4	599 ± 93	2.54	81	118.4 ± 7.1

PU/BSO5-1	321 ± 82	0.61	59	98.8 ± 5.6
PU/BSO5-2	283 ± 78	0.64	65	101.3 ± 2.6
PU/BSO5-3	377 ± 42	1.48	80	97.9 ± 1.3
PU/BSO5-4	357 ± 61	1.17	76	105.0 ± 6.6
PU/BSO10-1	346 ± 62	0.49	45	84.2 ± 8.4
PU/BSO10-2	338 ± 68	0.72	63	102.4 ± 2.8
PU/BSO10-3	443 ± 72	1.03	66	98.2 ± 4.7
PU/BSO10-4	433 ± 88	1.22	72	113.7 ± 2.4
PU/BSO15-1	460 ± 83	0.92	61	96.3 ± 6.1
PU/BSO15-2	620 ± 81	1.50	67	95.6 ± 7.2
PU/BSO15-3	675 ± 90	0.87	39	86.4 ± 3.3
PU/BSO15-4	794 ± 80	1.65	62	97.1 ± 1.4

In the study, the effect of flow rate and the distance between the needle and the collector on surface morphology were also investigated. When the flow rate was increased from 0.5 mL/h to 0.7 mL/h, nanofibers with larger diameters were produced (Figure 2), as expected. Also, with the increase in flow rate, the pore sizes of the nanofibrous mats were increased, nanofibers were flattened, and nanofiber web formation was observed. In electrospinning, if the flow rate is high, due to the greater volume of solution drawn from the needle tip, the jet needs longer time to dry. As a result, the solvents in the deposited fibers may not have enough time to evaporate. Evaporation of some amount of residual solvent from the fibers on the collector may cause the fibers to fuse together at contact points where they become flattened and form webs (Ramakrishna et al., 2005; Li and Wang, 2013, Baji et al., 2010). Although the increase of the fiber diameter is caused by flattening, the increase in the pore size might be associated with the dissolution of some fiber during solvent evaporation and the formation of new pores.

The distance between the needle and the collector also affect the nanofiber morphology and diameter. If the distance is short, the fiber cannot find enough time to solidify before reaching the collector. When the distance is increased, the polymer jet exposed to higher electrical forces, the flight time of the jet increases as a result, thinner nanofibers are obtained (Li and Wang, 2013). In this study, PU and PU/BSO nanofibrous mats were produced with different distances at 18 cm and 20 cm. It was seen that with the increasing distance, the nanofibrous mats with higher porosity, higher pore size, and thinner fibers were produced (Figure 3).

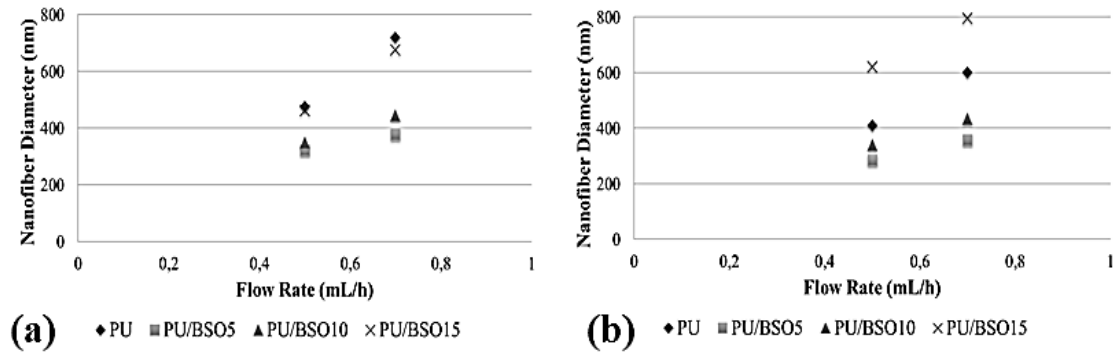

Figure 2:
The effect of flow rate on the diameters of nanofibers produced with different distances:a) 18 cm, b) 20 cm

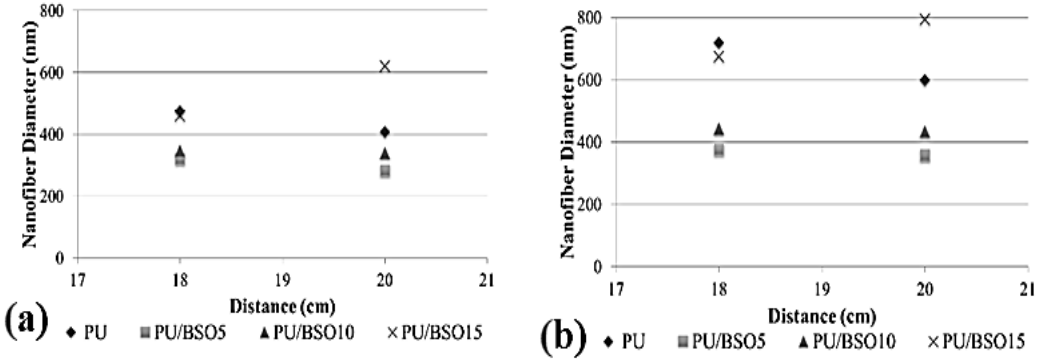

Figure 3:
The effect of distance on the diameters of nanofibers produced with different flow rates: a) 0.5 mL/h, b) 0.7 mL/h

Contact angle measurements give information about the surface characteristics of the materials such as, surface wettability, adhesion, hydrophobicity, absorption, etc. (Hsieh, 2001). In this study, all PU and PU/BSO nanofibrous mats showed contact angle values higher than 90° indicating that all the surfaces were hydrophobic due to the chemical structure of PU polymer. Pure PU nanofibrous mats produced with different flow rates and distances had contact angle values changing from 103.5° to 118.4°. The lowest contact angle was observed as 86.4° for the samples produced from the solutions containing 15% wt. BSO. Although, BSO has a hydrophobic nature, adding BSO into the nanofiber structure decreased the contact angle values. Contact angle values are dependent on the compounds present at the surface, the surface roughness, and the surface morphology. Surface morphology and roughness of the nanofibrous mats are affected by the diameter of the nanofibers, pore sizes and porosity of the nanofibrous mats. Highly porous surfaces show high contact angle due to the air pockets trapped under the liquid drop (Darmanin and Guittard, 2014). In the present study, pure PU nanofibrous mats had higher porosity compared to the PU/BSO nanofibrous mats (Table 3). Therefore, more porous surfaces produced from pure PU solutions, showed higher contact angle values. This proved that surface structure has a significant effect on the wettability of the nanofibrous mats.". FTIR analysis were performed in order to show the presence of BSO in the nanofibrous mats (Figure 4). FTIR analysis are not affected by the concentration of the spinning solution. Although, the concentration may affect the intensity of the peak, it doesn't affect the location of the peak. Therefore, FTIR spectrums of BSO, pure PU nanofibrous mat and PU/BSO nanofibrous mat were given in this study. The spectrum of pure PU exhibited peaks at 3327 cm^{-1}, 2954 cm^{-1},

2865 cm^{-1}, 1727 cm^{-1}, 1701 cm^{-1}, 1597 cm^{-1}, 1527 cm^{-1}, 1220 cm^{-1}, 1142 cm^{-1} and 770cm^{-1}. The peak at 3327 cm^{-1} is a characteristic broad of PU that corresponds with stretching vibration of the N-H in urethane groups and the peak at 1597 cm^{-1} and 1527 cm^{-1}shows the vibration of the NH stretch (Tang and Gao, 2017). The other absorption peaks of pure PU were observed at 2954 cm^{-1} and 2865 cm^{-1} that denote CH_2 asymmetric vibration and CH_3 symmetric vibration, respectively (Tijing et al., 2012). The peaks at 1701 cm^{-1} and 1727 cm^{-1} exhibit stretching vibration of carbonyl group (C=O) in hard segments and C-O vibration corresponding to alcohol groups were observed at 1220 cm^{-1}, 1142 cm^{-1}, 770cm^{-1} (Ayyar et al., 2017).

Triacylglycerol composition (TAG) is the main compound of oils and fats, comprising 96–98% of them. The dominant TAGs in black seed oil are mainly tri-linoleoyl, oleoyl-di-linoleoyl, palmitoyldi-linoleoyl, palmitoyl-oleoyllinoleoyl and dioleoyl-linoleoyl (Mazaheri et al., 2019). It was supported by the fatty acid composition of BSO results (Table 4). It is well known that TAGs response to characteristic peaks were at 3009 cm^{-1} (trans =C-H stretch), 2923 cm^{-1} (-CH_2 symmetrical stretching), 2854cm^{-1} (- CH_2 asymmetrical stretching), 1743 cm^{-1} (-C=O stretching of esters) and 1659 (-C=C asymmetrical stretching) due to the dominance of carbon chains in the unsaturated fatty acids (Nurrulhidayah et al. 2011; Kalhori et al., 2018; Yang et al., 2005). The PU/BSO nanofiber spectrum was similar to PU nanofiber spectrum. The peak at 3325 cm^{-1} and 2951 cm^{-1} related to stretching vibration of the N-H and C=N which are characteristic bond of PU. But, the peak at 2926 cm^{-1} and 2855 cm^{-1} were due to the presence of oil in the nanofiber.

Table 4. The main fatty acid composition of BSO

Components	Amount (%)
Linoleic acid (C18:2)	55.10 ± 4.00
Oleic acid (C18:1)	23.60 ±1.80
Palmitic acid (C16:1)	11.70 ± 1.00
Stearic acid (C18:0)	3.15 ± 0.24
Eicosenoic ccid (C20:3)	2.57 ± 0.01

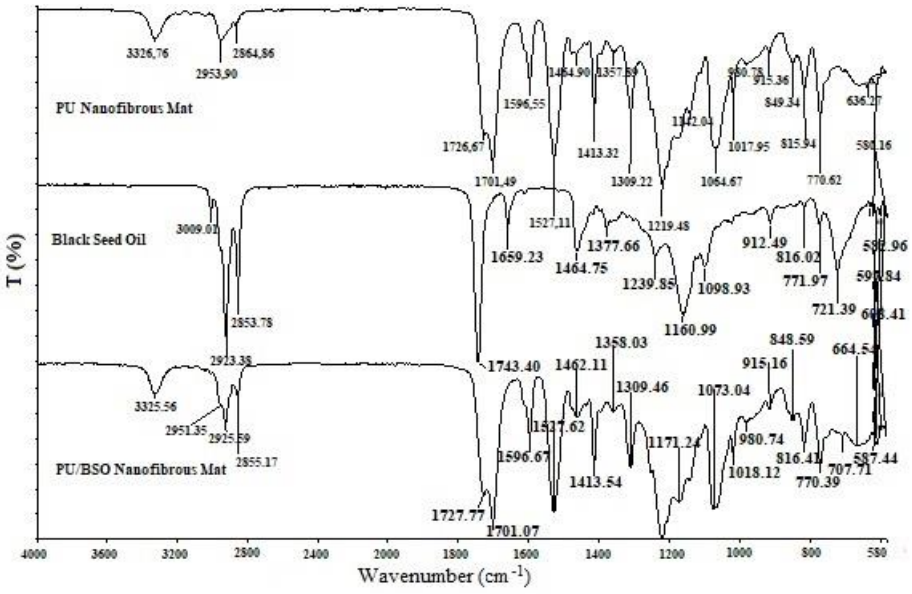

Figure 4:
FTIR spectra of the BSO, PU nanofibrous mat, and PU/BSO nanofibrous mat

4. CONCLUSION

BSO is widely used for medical applications due to its anti-inflammatory, and antimicrobial properties. PU is a biocompatible, non-toxic, and non-inflammatory polymer that has been intensively used in wound dressings. Polymeric nanofibers provide excellent surfaces for wound healing because of their unique properties.

In the study, PU and PU/BSO nanofibrous mats were produced by electrospinning. The effect of BSO content, and electrospinning parameters such as flow rate and spinning distance on the morphological properties of nanofibrous mats were investigated.

SEM results showed that pure PU nanofibers had diameters between 400-700 nm. With the increasing flow rate, diameters of the PU nanofibers were increased, whereas the diameters were decreased with the increasing spinning distance.

Depending on the BSO content in the polymer solution, the nanofiber diameters also increased due to the increase in viscosity. The lowest diameter was obtained with the samples produced from 5% wt. BSO containing solutions.

BSO addition also had an effect on the wettability of the nanofibrous mats. Although BSO has a hydrophobic nature, contact angle values were decreased with the increase in BSO content due to the surface morphology. This indicates that not only the chemical structure of the BSO, but also the porosity play an important role on wettability of the nanofibrous mats. FTIR results showed that, BSO was successfully loaded into the nanofibrous structure and it was compatible with PU.

It can be concluded that, PU/BSO nanofibrous mats can be promising for wound healing applications due to their high porosity, reasonable wetting property, and small fiber diameters.

REFERENCESS

1. Ahmad, A., Husain, A., Mujeeb, M., Khan, S. A., Najmi, A. K., Siddique, N. A., & Anwar, F. (2013) A review on therapeutic potential of Nigella sativa: A miracle herb, *Asian Pacific Journal of Tropical Biomedicine*, 3(5), 337–352. doi:10.1016/s2221-1691(13)60075-1

2. Akduman, C., Özgüney, I., & Kumbasar, E. P. A. (2016) Preparation and characterization of naproxen-loaded electrospun thermoplastic polyurethane nanofibers as a drug delivery system. *Materials Science and Engineering*, 64, 383–390. doi:10.1016/j.msec.2016.04.005

3. Akduman, C., & Kumbasar, E. P. A. (2017) Electrospun Polyurethane Nanofibers, *Aspects of Polyurethanes*. doi:10.5772/intechopen.69937

4. Aljabre, S. H. M., Randhawa, M. A., Akhtar, N., Alakloby, O. M., Alqurashi, A. M., & Aldossary, A. (2005) Antidermatophyte activity of ether extract of Nigella sativa and its active principle, thymoquinone, *Journal of Ethnopharmacology*, 101(1-3), 116–119. doi:10.1016/j.jep.2005.04.002

5. Almetwally, A. A., El-Sakhawy, El-shakankery, Elshakankery, M. H, & M., Kasem, M. (2017). Technology of nano-fibers: Production techniques and properties - critical review, Journal of the Textile Association, 78(1), 5-14.

6. Ayyar, M., Mani, M. P., Jaganathan, S. K., & Rathanasamy, R. (2017) Preparation, characterization and blood compatibility assessment of a novel electrospun nanocomposite comprising polyurethane and ayurvedic-indhulekha oil for tissue engineering applications. *Biomedical Engineering/ Biomedizinische Technik*. doi:10.1515/bmt-2017-0022

7. Baji, A., Mai, Y. W., Wong, S. C., Abtahi, M., & Chen, P. (2010) Electrospinning of Polymer Nanofibers: Effects on Oriented Morphology, Structures and Tensile Properties, *Composites Science and Technology*, 70, 703-718. doi: https://doi.org/10.1016/j.compscitech.2010.01.010

8. Burits, M. & Bucar, F. (2000) Antioxidant activity of *Nigella sativa* essential oil. Phytother. Res., 14: 323-328. doi:10.1002/1099-1573(200008)14:5<323::AID-PTR621>3.0.CO;2-Q

9. Chen, R., Morsi, Y., Patel, S., Ke, Q., & Mo, X. (2009) A novel approach via combination of electrospinning and FDM for tri-leaflet heart valve scaffold fabrication. *Frontiers of Materials Science in China*, 3(4), 359–366.doi:10.1007/s11706-009-0067-3

10. Chronakis, I. S. (2005) Novel nanocomposites and nanoceramics based on polymer nanofibers using electrospinning process—A review, *Journal of Materials Processing Technology*, 167(2-3), 283–293. doi:10.1016/j.jmatprotec.2005.06.053

11. Darmanin, T. & Guittard, F. (2014) Wettability of conducting polymers: from superhydrophilicity to superoleophobicity, *Progress in Polymer Science*, 39, 656-682. doi: http://dx.doi.org/10.1016/j.progpolymsci.2013.10.003

12. Demir, M. ., Yilgor, I., Yilgor, E., & Erman, B. (2002) Electrospinning of polyurethane fibers, *Polymer*, 43(11), 3303–3309. doi:10.1016/s0032-3861(02)00136-2

13. Detta, N., Errico, C., Dinucci, D., Puppi, D., Clarke, D. A., Reilly, G. C., & Chiellini, F. (2010) Novel electrospun polyurethane/gelatin composite meshes for vascular grafts, *Journal of Materials Science:Materials in Medicine*, 21(5), 1761–1769. doi:10.1007/s10856-010-4006-8

14. Düzyer, Ş. (2017) Fabrication Of Electrospun Poly (Ethylene Terephthalate) Scaffolds: Characterization And Their Potential On Cell Proliferation In Vitro, Tekstil Ve Konfeksiyon, 27(4), 334-341 WOS:000419066800002

15. Gali-Muhtasib, H., Diab-Assaf, M., Boltze, C., Al-Hmaira, J., Harting, R., Roessner, A., & Schneider-Stock, R. (2004) Thymoquinone extracted from black seed triggers apoptotic cell death in human colorectal cancer cells via a p53-dependent mechanism, Internatıonal Journal of Oncology, 25, 857-866 doi: 10.3892/ijo.25.4.857

16. Guo, H.-F., Li, Z.-S., Dong, S.-W., Chen, W.-J., Deng, L., Wang, Y.-F., & Ying, D.-J. (2012) Piezoelectric PU/PVDF electrospun scaffolds for wound healing applications. Colloids and Surfaces B: Biointerfaces, 96, 29–36.doi:10.1016/j.colsurfb.2012.03.014

17. Güzelsoy, P., Aydın, S., & Başaran, N. (2018) Çörek Otunun (Nigella Sativa L.) Aktif Bileşeni Timokinonun İnsan Sağlığı Üzerine Olası Etkileri, *Journal of Literature Pharmacy Sciences*, 7(2), 118-135. doi: 10.5336/pharmsci.2018-59816

18. Hacker, C., Karahaliloglu, Z., Seide, G., Denkbas, E. B., & Gries, T. (2013) Functionally modified, melt-electrospun thermoplastic polyurethane mats for wound-dressing applications. Journal of Applied Polymer Science, 131(8), n/a–n/a. doi:10.1002/app.40132

19. Hajhashemi, V., Ghannadi, A., & Jafarabadi, H. (2004) Black cumin seed essential oil, as a potent analgesic and antiinflammatory drug, *Phytotherapy Research*, 18(3), 195–199. doi:10.1002/ptr.1390

20. Hsieh, Y. (2001) Surface Characteristics of Polyester Fibers: Surface Characteristics of Fibers and Textiles, Editors: Pastore, C. M., Kiekens, P., Markel Dekker Inc., p.33-57,USA

21. Huang, Z.-M., Zhang, Y.-Z., Kotaki, M., & Ramakrishna, S. (2003) A review on polymer nanofibers by electrospinning and their applications in nanocomposites, *Composites Science and Technology, 63(15), 2223–2253.* doi:10.1016/s0266-3538(03)00178-7

22. Kalhori, F., Arkan, E., Dabirian, F., Abdi, G., & Moradipour, P. (2018) Controlled Preparation and Characterization of Nigella Sativa Electrospun Pad for Controlled Release. *Silicon*. doi:10.1007/s12633-018-9931-z

23. Li, Z., & Wang, C. (2013) One-Dimensional nanostructures: Electrospinning Technique and Unique Nanofibers, *SpringerBriefs in Materials*, 15-25. doi:10.1007/978-3-642-36427-3

24. Liakos, I., Holban, A., Carzino, R., Lauciello, S., & Grumezescu, A. (2017) Electrospun Fiber Pads of Cellulose Acetate and Essential Oils with Antimicrobial Activity. Nanomaterials, 7(4), 84. doi:10.3390/nano7040084

25. Ma, Z., Kotaki, M., Yong, T., He, W., Ramakrishna, S. (2005) Surface Engineering of Electrospun Polyethylene Terephthalate (PET) Nanofibers Towards Development of a New Material for Blood Vessel Engineering, *Biomaterials*, 26, 2527-2536. doi:10.1016/j.biomaterials.2004.07.026

26. Majdalawieh, A. F., Fayyad, M. W., & Nasrallah, G. K. (2017) Anti-cancer properties and mechanisms of action of thymoquinone, the major active ingredient of Nigella sativa, *Critical Reviews in Food Science and Nutrition*, 57(18), 3911–3928. doi:10.1080/10408398.2016.1277971

27. Manikandan, A., Mani, M. P., Jaganathan, S. K., Rajasekar, R., & Jagannath, M. (2017) Formation of functional nanofibrous electrospun polyurethane and murivenna oil with improved haemocompatibility for wound healing. Polymer Testing, 61, 106–113. doi:10.1016/j.polymertesting.2017.05.008

28. Mi, H.-Y., Jing, X., Jacques, B. R., Turng, L.-S., & Peng, X.-F. (2013) Characterization and properties of electrospun thermoplastic polyurethane blend fibers: Effect of solution rheological properties on fiber formation, *Journal of Materials Research*, 28(17), 2339–235. doi:10.1557/jmr.2013.115

29. Mi, H.-Y., Salick, M. R., Jing, X., Crone, W. C., Peng, X.-F., & Turng, L.-S. (2014) Electrospinning of unidirectionally and orthogonally aligned thermoplastic polyurethane nanofibers: Fiber orientation and cell migration. *Journal of Biomedical Materials Research Part A*, 103(2), 593–603. doi:10.1002/jbm.a.35208

30. Nurrulhidayah, A.F., Che-Man, Y.B., Al-Kahtani, H.A., & Rohman, A. (2011) Application of FTIR spectroscopy coupled with chemometrics for authentication of Nigella sativa seed oil, *Spectroscopy*, 25, 243–250. doi: 10.3233/SPE-2011-0509

31. Pant, H. R., Pokharel, P., Joshi, M. K., Adhikari, S., Kim, H. J., Park, C. H., & Kim, C. S. (2015) Processing and characterization of electrospun graphene oxide/polyurethane composite nanofibers for stent coating. *Chemical Engineering Journal*, 270, 336–342. doi:10.1016/j.cej.2015.01.105

32. Rajendran, S. (2009) Advance textiles for wound care, *CRC Press, Woodhead Publishing in Textiles*, p:55, UK, ISBN: 1420094890,9781420094893

33. Ramakrishna, S., Fujihara, K., Teo, W. E., Lim, T. C., Ma, Z. (2005) An Introduction to Electrospinning and Nanofibers, *World Scientific Publishing Company*, 90-101,USA, ISBN: 981-256-415-2

34. Randhawa, M., Alenazy, A., Alrowaili, M., & Basha, J. (2017) An active principle of Nigella sativa L, thymoquinone, showed significant antimicrobial activity against anaerobic bacteria, *Journal of Intercultural Ethnopharmacology, 6(1), 97.* doi:10.5455/jice.20161018021238

35. Rieger, K. A., & Schiffman, J. D. (2014) Electrospinning an essential oil: Cinnamaldehyde enhances the antimicrobial efficacy of chitosan/poly(ethylene oxide) nanofibers. Carbohydrate Polymers, 113, 561–568.doi:10.1016/j.carbpol.2014.06.075

36. Saha, K., Butola, B. S., & Joshi, M. (2014) Drug release behavior of polyurethane/clay nanocomposite: Film vs. nanofibrous web. Journal of Applied Polymer Science, 131(19). doi:10.1002/app.40824

37. Sharmin, E., & Zafar, F. (2012) Polyurethane: An Introduction. Polyurethane. *Intechopen*, doi:10.5772/51663

38. Tan, L., Hu, J., Huang, H., Han, J., & Hu, H. (2015) Study of multi-functional electrospun composite nanofibrous mats for smart wound healing. International Journal of Biological Macromolecules, 79, 469–476.doi:10.1016/j.ijbiomac.2015.05.014

39. Tang, Q., & Gao, K. (2017) Structure analysis of polyether-based thermoplastic polyurethane elastomers by FTIR, ^{1}H NMR and ^{13}C NMR, *International Journal of Polymer Analysis and Characterization*, 22(7), 569–574. doi:10.1080/1023666x.2017.1312754

40. Teo, W. E., & Ramakrishna, S. (2006) A review on electrospinning design and nanofibre assemblies. *Nanotechnology*, 17(14), 89–106. doi:10.1088/0957-4484/17/14/r01

41. Theron, S. A., Zussman, E., & Yarin, A. L. (2004) Experimental investigation of the governing parameters in the electrospinning of polymer solutions, *Polymer*, 45(6), 2017–2030. doi:10.1016/j.polymer.2004.01.024

42. Theron, J. P., Knoetze, J. H., Sanderson, R. D., Hunter, R., Mequanint, K., Franz, T., & Bezuidenhout, D. (2010) Modification, crosslinking and reactive electrospinning of a thermoplastic medical polyurethane for vascular graft applications. *Acta Biomaterialia*, 6(7), 2434–2447. doi:10.1016/j.actbio.2010.01.013

43. Tijing, L., Ruelo, M., Amarjargal, A., Pant, H., Park, C., Kim, D., Kim C. (2012) Antibacterial and superhydrophilic electrospun polyurethane nanocomposite fibers containing tourmaline nanoparticles, *Chemical Engineering Journal*, 197, 41–48. doi: 10.1016/j.cej.2012.05.005

44. Yang, H., Irudayaraj, J., & Paradkar, M. M. (2005) Discriminant analysis of edible oils and fats by FTIR, FT-NIR and FT-Raman spectroscopy, *Food Chem*,93(1), 25-32. doi:10.1016/j.foodchem.2004.08.039

45. Yeganeh Mazaheri, Mohammadali Torbati, Sodeif Azadmard-Damirchi & Geoffrey P. Savage (2019) A comprehensive review of the physicochemical, quality and nutritional properties of Nigella sativa oil, *Food Reviews International*, 35(4) 342–362. doi:10.1080/87559129.2018.1563793

46. Yuan, Y., & Lee, T. R. (2013) Contact Angle and Wetting Properties, *Springer Series in Surface Sciences*, 3–34. doi:10.1007/978-3-642-34243-1_1

47. Wang, Y., Hao, J., Huang, Z., Zheng, G., Dai, K., Liu, C., & Shen, C. (2018) Flexible electrically resistive-type strain sensors based on reduced graphene oxide-decorated electrospun polymer fibrous mats for human motion monitoring. Carbon, 126, 360–371. doi:10.1016/j.carbon.2017.10.034

48. Wen, P., Zhu, D.-H., Wu, H., Zong, M.-H., Jing, Y.-R., & Han, S.-Y. (2016). Encapsulation of cinnamon essential oil in electrospun nanofibrous film for active food packaging. Food Control, 59, 366–376. doi:10.1016/j.foodcont.2015.06.005

49. Zaoui, A., Cherrah, Y., Mahassini, N., Alaoui, K., Amarouch, H., & Hassar, M. (2002) Acute and chronic toxicity of Nigella sativa fixed oil, *Phytomedicine, 9(1), 69–74.* doi:10.1078/0944-7113-00084

50. Zhu, G., Kremenakova, D., Wang, Y., Militky, J. (2015) Air Permeability of Polyester Nonwoven Fabrics, *AUTEX Research Journal*, 15(1), 8-12. 11. doi: 10.2478/aut-2014-0019